Atom Indonesia

Comparative Analysis of Turbulence Models for Thermal-Hydraulic Simulations in Aqueous Homogeneous Reactors

D. M. Pérez[1,2*]**, A. G. Rodríguez**[1,2]**, D. E. M. Lorenzo**[3]**, C. A. B. de Oliveira Lira**[2]

[1]*Departamento de Energia Nuclear, Universidade Federal de Pernambuco (UFPE), Cidade Universitária, Avenida Professor Luiz Freire 1000, Recife, PE, Brasil*
[2]*Centro Regional de Ciências Nucleares (CRCN-NE/CNEN), Cidade Universitária, Avenida Professor Luiz Freire 200, Recife, PE, Brasil*
[3]*University of Havana, Avenida Salvador Allende y Luaces, Quinta de Los Molinos, Plaza de la Revolución, 10400, Havana, Cuba*

ARTICLE INFO

ABSTRACT

This article presents a comparative study of various turbulence models applied in the context of thermal-hydraulic simulations for liquid fuel reactors, specifically Aqueous Homogeneous Reactors (AHR) using Computational Fluid Dynamics. The objective was to assess the suitability of the turbulence models by comparing their results with data obtained from Large Eddy Simulation (LES). For that purpose, was compared the flow behavior predicted using the k-ε, SST, GEKO, DES, SBES, and LES turbulence models. The calculations were carried out in a simplified computational model derived from a pre-existing three-dimensional AHR conceptual design. By utilizing this simplified model, the study aimed to focus on the computational differences between the turbulence models, while minimizing the influence of other factors. The calculation results revealed that the k-ε model exhibited significant discrepancies with the LES, with relative differences for the fuel solution maximum temperature reaching up to 75 %. Among the remaining RANS models, the Shear Stress Transport (SST) model demonstrated the best compromise between accuracy and computational efficiency, with differences below 5 % and requiring only 1/5th of the time, compared to the LES model. The Scale-Resolving Simulation (SRS) models, DES and SBES, provided a more comprehensive description of flow behavior and results closer to LES, albeit with higher computational demands. Between these two models, only the DES model exhibited relative differences below or equal to 1 % compared to the LES model for the studied thermohydraulic parameters.

INTRODUCTION

In recent years, several alternative technologies to produce ^{99}Mo and other radioisotopes have attracted the attention of the scientific community, one of these technologies are the liquid fuel reactors. Specifically, the Aqueous Homogeneous Reactors (AHR), have drawn attention due to their advantages in comparison with heterogeneous reactors: low cost, small critical mass, inherent passive safety, and simplified fuel handling, processing, and purification characteristics [1]. This interest has led to the development of a group of projects based on this technology around the world.

The Russian Federation decided to build the ARGUS-M, a 50 kWth AHR, capable of producing 250 six days Curie per week of ^{99}Mo. The Nuclear Power Institute of China (NPIC) finished the design of the Medical Isotope Production Reactor (MIPR) in 2015. It has a projected production capacity of 2000 six days Curie per week of ^{99}Mo, in addition to obtaining ^{131}I and ^{89}Sr [2]. Other non-reactor-based methods of producing ^{99}Mo on smaller scales have been proposed to diversify the conventional supply chain and meet local and regional demands. Perhaps the most promising variant is the use of an accelerator-driven Aqueous Homogeneous Subcritical System (AHSS), such as the design proposed by SHINE Medical Technologies. This system is under construction and it is planned to start producing 4000 six days Curie of ^{99}Mo in the US with eight units

[3,4]. In Indonesia, the National Nuclear Energy Agency (BATAN) is currently implementing a similar [99]Mo producing system. The system is constituted by a subcritical assembly that operates driven by an external neutron source. This source can be a neutron generator or another type of accelerator-based neutron source. The subcritical assembly fueled with uranyl nitrate, called Subcritical Assembly for [99]Mo Production (SAMOP) has been designed and will be developed further at the Center for Accelerator Science and Technology (CAST) [5-8].

Although the use of AHR and AHSS in the production of medical isotopes represents an attractive alternative compared to the traditional method of irradiating solid targets in heterogeneous reactors, the commercial deployment of this technology requires substantial research, development, and demonstration of the nuclear safety characteristics. Considering the lack of experimental facilities and the costs associated with their construction, the use of the multi-physics computational simulation could provide a cost-effective and accurate initial alternative in the pursuit of improvements in the efficiency, safety, and reliability of these systems. It is important to highlight that, among the multi-physics computational simulations necessary for the study of these systems (thermal-hydraulics, neutronics, and thermomechanics), it has been identified that significantly larger errors are usually introduced from the thermal-hydraulics rather than from the other physics simulations [9]. Several unique and challenging features of the thermal-hydraulic modeling of liquid fuel reactors are responsible [10]. Among them, is the use of inaccurate or inappropriate models when attempting to predict the effects of turbulence. Capturing these effects is an essential component for accurate thermal-hydraulic modeling using Computational Fluid Dynamics (CFD) codes [11]. The most commonly used turbulence models are the Reynolds-Averaged Navier-Stokes (RANS) models, specifically the k-ε models. The k-ε model is a two-equation model widely used to predict turbulent momentum and turbulent kinetic energy on a simple but practical level. It is found to be fairly accurate for most applications, but its performance can degrade in certain cases due to its simplified assumptions [12,13]. Other RANS turbulence models are the zero-equation model, the one-equation model, the two-equation models (k–ε models, k–ω models), and finally the seven-equation models, also known as the Reynolds stress models [11]. Overall, the selection of the appropriate turbulence model is dependent on the application requirements. For most applications, the k-ε and the k-ω models will be

sufficient. However, for more complex flows, more advanced models may be needed. In these scenarios, more accurate methods, such as Large Eddy Simulations (LES) or Direct Numerical Simulation (DNS), must be employed [13]. These models are known as Scale-Resolving Simulation (SRS) models.

The use of SRS modeling provides a broader range of applicability and more accurate results compared to RANS modeling. The broader applicability and improved accuracy of these models make them excellent choices for studying the complex fluid dynamics phenomena found in nuclear facilities. This increase in the utilization of SRS models has been observed through a growing number of articles in recent years, particularly in terms of their comparison with results obtained using RANS models [14-24]. Additionally, they have been employed as substitutes for experimental results in cases where budget constraints limited the feasibility of experimentation or where a reduction in the number of experimental scenarios to evaluate was required. This scenario specifically applies to AHR, as the availability of experimental facilities for these systems is extremely limited or virtually non-existent [25].
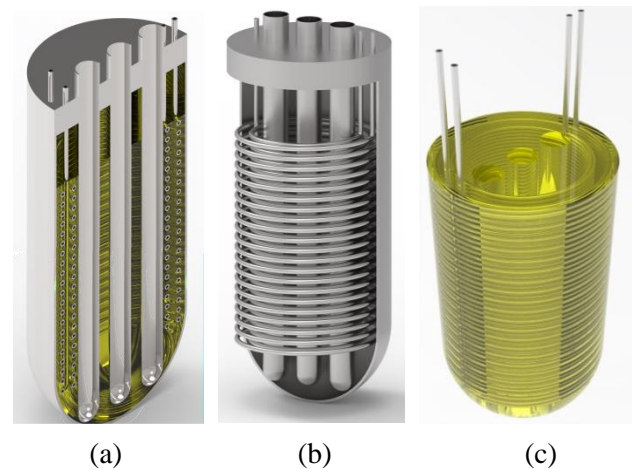

(a)   (b)   (c)

Fig. 1. Full three-dimensional AHR conceptual design (a) Axial section of the assembly core. (b) View of the vessel's internal structural parts including the core channels, the coiled cooling pipes, and the vessel walls. (c) Fuel solution, and the coiled cooling pipes.

Nevertheless, both LES and DNS are computationally expensive and are generally limited to low Reynold number flows over simple geometries, as the computational resources needed and the effort put into them are still too excessive for most practical uses [12,13]. Therefore, in this work, various turbulence models were employed to predict the thermal-hydraulic behavior of a simplified AHR computational model. The AHR computational model is a simplification of a full three-dimensional

AHR conceptual design (Fig. 1) previously studied using k–ε and k–ω turbulence models [25,26]. The simplification is carried out in order to avoid other effects and to focus on the computational differences between the models only. The calculations were carried out using the CFD code ANSYS CFX, version 2023 R1. The main aim was to determine the most suitable turbulence model via comparison with the SRS results, which is considered the most accurate approach to turbulent flow simulation. This is of particular interest to find a compromise between simulation time and accurate results. For that, was compared the flow behavior predicted using each of the studied models (k-ε, SST, GEKO, DES, SBES, and LES models).

MATERIALS AND METHODS

In the past, RANS models were almost the only option to solve engineering problems of turbulent flows using CFD analysis. In recent years, with the rapid increase in computing power, the SRS models have seen an increase in usage for accurate flow description, where previously RANS methods were typically applied. Even though, these methods (specifically, DNS and LES) remain computationally impractical for all but the simplest configurations/geometries. Therefore, to carry out the comparative studies proposed in this paper, a simplified model of the AHR model studied in [25,26] was used (Fig. 2).
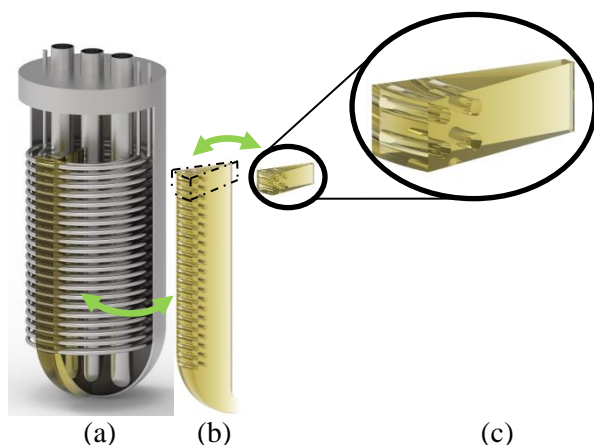

Fig. 2. CFD geometry of the AHR. (a) Full three-dimensional AHR conceptual design (with the 20° section - AHR model highlighted) (b) 20° section - AHR model in [25,26] (c) Simplified model used in this paper.

The original geometrical conceptual design consists of a stainless-steel cylindrical vessel with a hemispherical bottom filled to a critical state with a low-enriched uranyl sulfate solution. Surrounding the vessel there is a graphite reflector that is horizontally encompassed by a borated polyethylene shield. Placed inside the vessel, there are two coiled-tube heat exchangers and three channels. The central channel has an experimental purpose, whereas the other two channels are intended for poison rods. In the simplified model used in this paper, many of these features are ignored taking into consideration that the objective of the study is to focus only on the computational differences between the turbulence models. Fig. 3 shows the main dimensions of the computational model used. In [25,26] are explained, described, and discussed the selection of the numerical models, thermal and material properties correlations, boundary conditions, solution parameters, geometrical and material approximations, and other modeling-related topics.
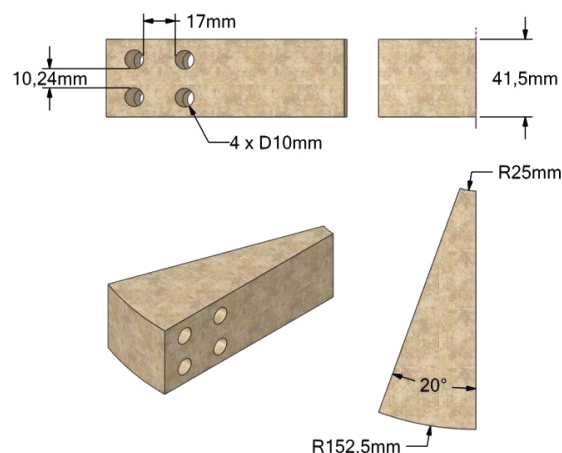

Fig. 3. Dimensions of the simplified model.

The tested RANS turbulence models in this study are the following:
(1) k-ε model;
(2) k-ω (Generalized) GEKO model (CJET=0.9, CNW=0.5, CSEP=1.75); and
(3) Shear Stress Transport (SST) model.
The studied SRS models are:
(1) Detached Eddy Simulation (DES);
(2) Stress Blended Eddy Simulation (SBES); and
(3) LES with the Wall-Adapting Local Eddy-Viscosity (WALE) model.

Three computational meshes (Fig. 4) were developed: (1) $2.74 \cdot 10^4$ elements ($Y^+ \sim$ 20-30) mesh for the k-ε model, (2) $2.02 \cdot 10^5$ elements ($Y^+ \leq 1$) mesh for the GEKO and SST models and, (3) $1.14 \cdot 10^6$ elements ($Y^+ \leq 1$) mesh for the SRS models (DES, SBES, and LES). The developed computational meshes meet the requirements and good practices established for simulations using RANS and SRS [27,28]. Additionally, was determined the appropriate temporal resolution to achieve a Courant number of CFL ≈ 1 [27]. Transient calculations with the SRS models were carried out during 200 seconds of flow in order to build accurate statistics.
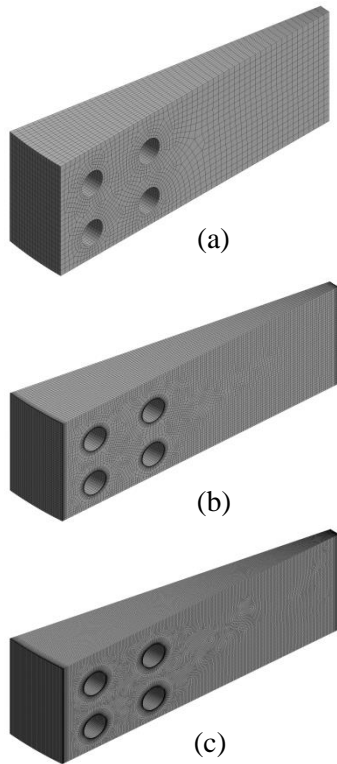
Fig. 4. Computational meshes. (a) k-ε model
(b) GEKO and SST models (c) SRS models.

A no-slip boundary condition was applied to the walls and the coiled cooling pipes. The amount of free convective heat transfer from the fuel solution to the walls and the cooling pipes were set using the appropriate correlations. Symmetry conditions were used in the vertical plane faces of the computational model and the degassing condition at the top. The simulations were done using a volumetric heat generation rate represented using an energy liberation profile obtained through a neutronic-thermal-hydraulics coupling [25,26]. The convergence criteria for the mass, momentum, energy, and turbulence RMS (Root Mean Square) Residuals were set to 10^{-6}; further refinement of the convergence criteria did not give any accuracy to the solutions.

RESULTS AND DISCUSSION

In order to assess the most appropriate turbulence model by comparing it with the SRS results, a series of thermohydraulic parameters obtained from the CFX simulation were taken into consideration. The key parameters that were taken into consideration included the maximum and average fuel solution temperatures, the average velocities of the fuel solution and gas bubbles, and the gas volume fraction within the fuel solution. Firstly, an assessment of the global parameters will be conducted to eliminate models that deviate significantly from the SRS results. Once this step is

finished, the differences and similarities between the remaining models will be evaluated.

As the first step, the temperature parameter was evaluated. Fig. 5 shows the maximum and average values for each turbulence model. As depicted in Figure 5, it is evident that, except for the k-ε model, the other models under investigation exhibit results that closely align with the simulation using LES, which is considered the most accurate for turbulent flow simulation in this research. The relative difference between the k-ε and LES models was found to be 75 % for the average temperature and 32 % for the maximum temperature. In the case of the other models examined, the maximum relative difference observed was 5 % for the maximum temperature in both the SST and GEKO models.
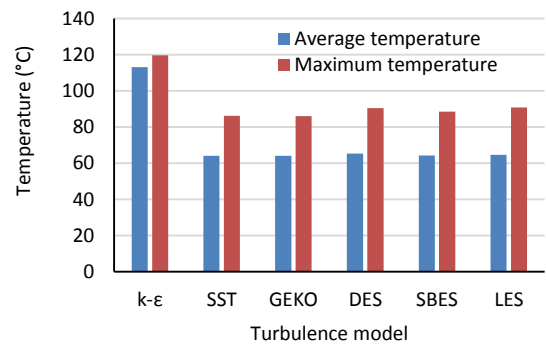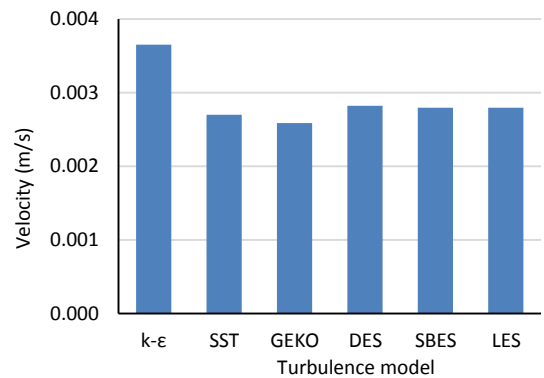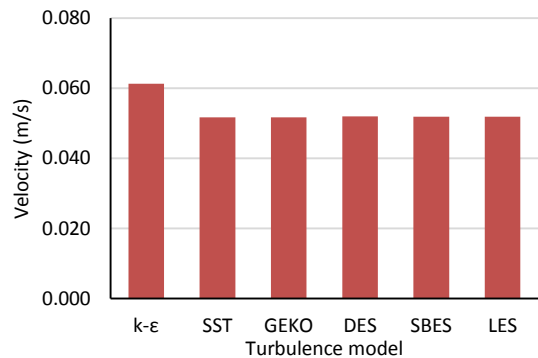

Fig. 5. Maximum and average temperature values for each turbulence model.

(a)

(b)

Fig. 6. Average velocities of the (a) fuel solution and (b) gas bubbles for each turbulence model.

The next step was evaluating the average velocities of the fuel solution and gas bubbles. As observed in Fig. 6, a behavior similar to that of the temperature was obtained. The relative difference between the k-ε and LES models was found to be 31 % for the average fuel solution velocity and 18 % for the average gas bubbles velocity. In the case of the other models examined, the maximum relative difference observed was 7 % for the average fuel solution velocity using the GEKO model.

Then, the gas volume fraction within the fuel solution was evaluated. Fig. 7 shows this result for each turbulence model. As observed, the k-ε model tends to underestimate the gas volume fraction, whereas the other RANS models tend to overestimate it. Despite these differences, the relative differences with the LES model do not exceed 1 %. The SRS models do not differ from each other.
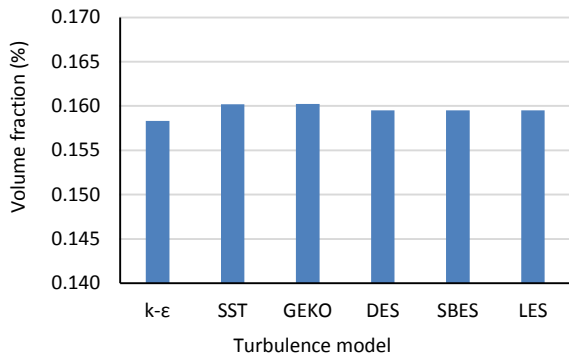

Fig. 7. Gas volume fraction within the fuel solution.

The next step was evaluating the degree of turbulent structure resolved with each SRS model. For that was studied the courant number field around the pipes with an iso-surface of Q-criterion at 1.0 s^{-2} (Fig. 8). The Q-criterion method, which is widely utilized in SRS [29], is a technique employed in the

visualization and analysis of turbulent flows. Its primary purpose is to identify and visualize regions of intense turbulence as well as the formation of coherent structures, such as vortices and mixing zones, (values of Q > 0 identify vortical structures). The differences in flow field prediction between the RANS and SRS models are quite apparent. It is evident that the SRS approach yielded a more realistic description of the flow pattern between the pipes, although at the cost of longer computation times compared to RANS models, typically ranging from four to five times higher (Table 1). No significant differences are observed among the three SRS models, as they resolve approximately the same level of turbulent structure. Table 2 presents a summary of the relative differences obtained for each thermohydraulic parameter studied when compared to the LES model. These relative differences highlight each model's performance relative to the LES model, with lower values indicating closer agreement.

Table 1. Normalized simulation time.

Turbulence model	Simulation time
k-ε	1.0
SST	6.1
GEKO	6.2
DES	28.3
SBES	28.4
LES	29.2

Table 2. The relative difference with the LES model.

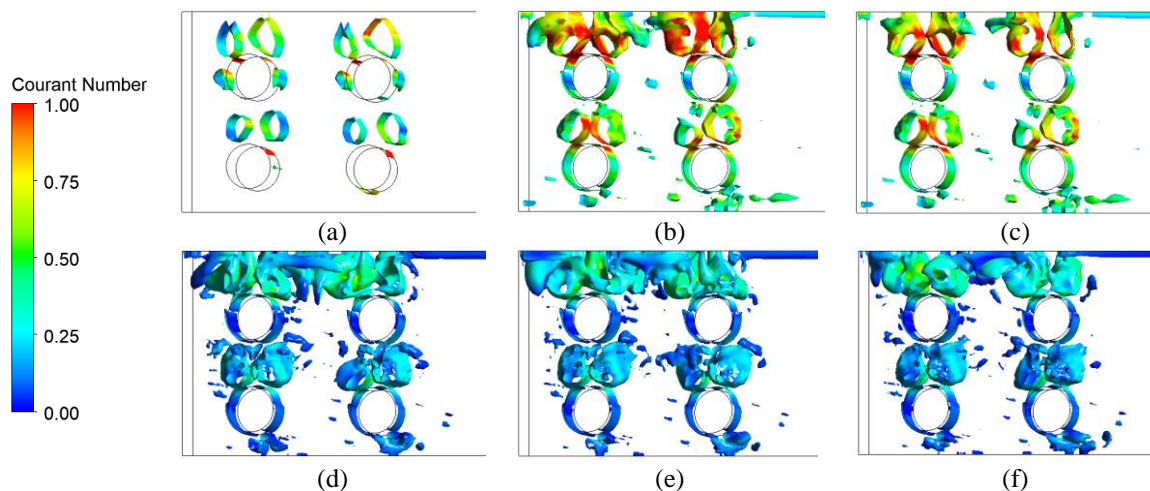| Turbulence model	Average temperature	Maximum temperature	Average fuel solution velocity	Average gas bubbles velocity	Gas volume fraction
k-ε	75.03 %	31.77 %	30.68 %	18.05 %	-0.73%
SST	-0.90 %	-5.16 %	-3.36 %	-0.47 %	0.43%
GEKO	-0.86 %	-5.38 %	-7.42 %	-0.48 %	0.46%
DES	1.00 %	-0.50 %	0.92 %	0.18 %	0.00%
SBES	-0.52 %	-2.64 %	0.01 %	-0.13 %	0.00%

Fig. 8. Courant number field around the pipes with iso-surface of Q-criterion at 1.0 s^{-2}. (a) k-ε, (b) SST, (c) GEKO, (d) DES, (e) SBES, and (f) LES turbulence models.

As previously discussed, only the k-ε model presents results that deviate significantly from the SRS results. Therefore, the k-ε model will be excluded from the subsequent tasks. Based on the analysis of the presented results, it can be inferred that among the studied parameters, the maximum temperature and the average fuel solution velocity are the most influenced by the turbulence model selection. Consequently, the subsequent studies will focus specifically on these parameters.

The calculated velocity profile around the pipes on a plane at the center of the section is shown in Fig. 9 for each turbulence model. It should be noted that the velocities displayed in Fig. 9 correspond to either the instantaneous velocities or the transient average velocities, depending on the turbulence model (RANS or SRS). This figure showcases significant features anticipated in this system based on previous studies, including the presence of large recirculating eddies in the area between the pipes. Within the remaining computational domain, a clear and consistent pattern of organized and laminar flow is observed. While the movement and location of the eddies exhibit a similar pattern, it is noticeable that the RANS models consistently underestimate the results obtained from the SRS models.
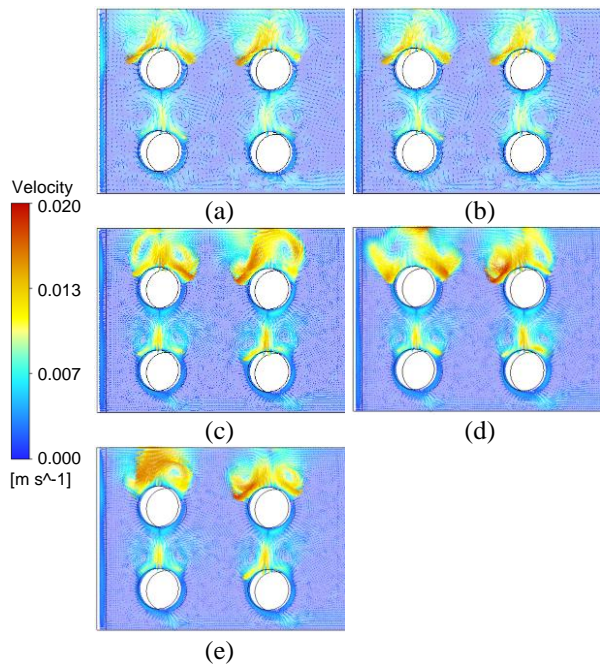

Fig. 9. Fuel solution velocity vectors profile around the pipes on a plane at the center of the section for the (a) SST, (b) GEKO, (c) DES, (d) SBES, and (e) LES turbulence models.

In Fig. 10, the temperature contours of the fuel solution for the studied turbulence models are displayed. It can be observed that the two RANS models exhibit similar behaviors to each other, with absolute values lower than the estimations of the SRS models. The SRS models also yield similar results to each other, providing a more detailed depiction of the fluid recirculation behavior at the top of the pipes.
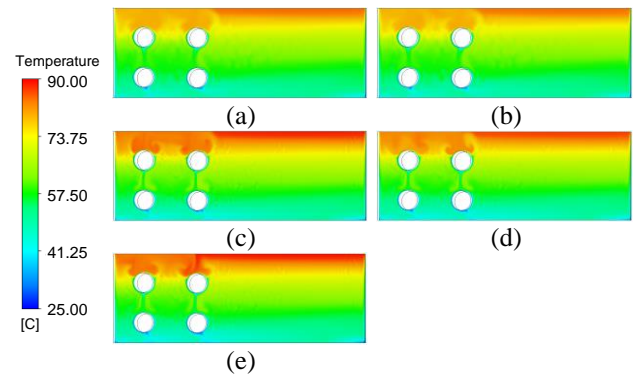

Fig. 10. Fuel solution temperature contours for the (a) SST, (b) GEKO, (c) DES, (d) SBES, and (e) LES turbulence models.

The results obtained in this study are relevant for understanding the behavior of the turbulence models in multiphase media in which heat transfer and fluid motion are governed by natural convection. The results obtained in this paper highlight the need to use more advanced approaches, such as SRS models, for a more accurate description of the turbulence in this system.

The observed differences in results among the turbulence models can be attributed to several key factors. Firstly, it was observed that the k-ε model, which is the most commonly used turbulence model in industrial applications, presents notable deviations from the LES results. These deviations can be linked to its simplistic representation of turbulence, particularly its limitations in handling complex flow phenomena, such as swirling or recirculating flows present in the AHR system. In addition, the k-ε model only models heat transfer in the near-wall region, unlike the other turbulence models considered that are capable of resolving heat transfer within the boundary layer. On the other hand, the other two RANS models (SST and GEKO) tend to underestimated the results by at least 5 % because they rely on steady-state assumptions and often struggle to capture unsteady or transitional behaviors seen in natural convection. These results are consistent with previous studies that have demonstrated the superiority of SRS models over RANS in turbulent flow simulation. This study extends that knowledge by comparing different SRS models with each other and showing that they present a similar degree of turbulent structure

resolved. This is crucial in accurately simulating the natural convection and multiphase flow behaviors inherent in AHR systems. For example, the DES model obtained relative differences below or equal to 1 % compared to the LES model for the thermohydraulic parameters studied. Overall, these differences stem from the inherent characteristics and mathematical formulations of each model, underlining the importance of selecting an appropriate turbulence model tailored to the complexity of the flow phenomena under investigation.

Finally, it is important to highlight the limitations of the study carried out in this paper. These are fundamentally related to the utilization of a simplified computational model with a specific geometry. Therefore, the results and conclusions may not be directly applicable to other AHR configurations. For future investigations, it would be interesting to evaluate the applicability of the models in the complete three-dimensional conceptual design, to validate and generalize these findings.

CONCLUSION

This paper delves into the study of the influence of RANS and SRS turbulence models in computational fluid dynamics simulations, specifically focusing on their impact on the thermal-hydraulic simulation. The main objective is to find a compromise between simulation time and accurate results, which is of particular interest in practical applications. For this purpose, the k-ε, SST, GEKO, DES, SBES, and LES turbulence models were employed to predict the thermal-hydraulic behavior of a simplified computational model of an AHR. The simplified model was derived from a pre-existing full three-dimensional conceptual design of the AHR. By using this simplified model, the study aimed to focus solely on the computational differences between the turbulence models and minimize other potential influences. The main thermal-hydraulic parameters studied during the investigation were the maximum and average fuel solution temperatures, the average velocities of the fuel solution and gas bubbles, and the gas volume fraction within the fuel solution.

It has been confirmed that the k-ε model offers the most time-efficient approach, demonstrating the shortest computation time compared to all the evaluated models. However, it is important to highlight that the k-ε turbulence model produced the largest deviations from the LES results, with differences of up to 75 %. Among the remaining RANS models, the SST model emerges as the most accurate and cost-effective option, with deviations of up to 5 % from the reference solution.

Furthermore, this model boasts an acceptable computational time, requiring only 1/5th of the resources compared to the LES model. In contrast, the SRS approaches provided a more comprehensive description of the flow field, including the resolution of turbulent structures, albeit they come at the cost of four to five times longer computation times than RANS models. The hybrid SRS models (DES and SBES) achieved results closer to LES than the RANS models, as expected. Among these two models, only the DES model exhibited relative differences below or equal to 1 % compared to the LES model for the studied thermohydraulic parameters.

AUTHOR CONTRIBUTION

D. Milian Pérez and A. Gámez Rodríguez conceived the presented idea, developed the theory, performed the computational calculations, and wrote the manuscript. D. E. Milian Lorenzo and C. A. Brayner de Oliveira Lira supervised the findings of this work. All authors read and approved the final version of the paper.

REFERENCES

1. IAEA, Homogeneous Aqueous Solution Nuclear Reactors for the Production of Mo-99 and Other Short Lived Radioistotopes, Vienna, 2008.

2. National Academies of Sciences Engineering and Medicine, *Opportunities and Approaches for Supplying Molybdenum-99 and Associated Medical Isotopes to Global Markets*, Proceedings of a Symposium, National Academies Press, Washington, DC (2018).

3. G. Piefer, K. M. Pitas, E. N. V. Abel *et al., Mo-99 Production using a Subcritical Assembly,* 1st Annual Molybdenum-99 Topical Meeting, Santa Fe, New Mexico, 2011.

4. N. Williams, Milwaukee Bus. J. (2018).

5. M. I. Farezza W and Syarip, J. Phys.: Conf. Ser. **1090** (2018) 012013.

6. F. Yassar, A. W. Harto and Syarip, J. Phys.: Conf. Ser. **1080** (2018) 012021.

7. Syarip, M. Rosyid, Dewita *et al.,* J. Phys.: Conf. Ser. **1280** (2019) 022070.

8. G. Abrar, Sihana and Syarip, Nucl. Eng. Des. **383** (2021) 111428.

9. M. E. Tano and P. Rubiolo, Energies **15** (2022) 6861.

10. N. R. Brown, D. J. Diamond, S. Bajorek *et al.*, Nucl. Technol. **206** (2020) 322.

11. ANSYS, Ansys CFX-Solver Theory Guide, ANSYS, Inc., 2023.

12. A. Dewan, Tackling Turbulent Flows in Engineering, Springer-Verlag, Berlin Heidelberg (2011).

13. S. N. A Yusof, Y. Asako, N. A. C. Sidik *et al.,* CFD Lett. **12** (2020) 83.

14. R. Ji, P.J. Wenig, S. Kelm *et al.,* Ann. Nucl. Energy **181** (2023) 109563.

15. H. Ju, H. Yu, M. Wang *et al.,* Ann. Nucl. Energy **161** (2021) 108474.

16. A. Fregni, D. Angeli, A. Cimarelli *et al.,* Nucl. Eng. Des. **389** (2022) 111597.

17. J. Feng, M. Acton, E. Baglietto *et al.*, Ann. Nucl. Energy **140** (2020) 107298.

18. A. Laureau, A. Bellè, M. Allibert *et al.*, Ann. Nucl. Energy **177** (2022) 109265.

19. Y. Wang, M. Wang, J. Zhang *et al.,* Ann. Nucl. Energy **159** (2021) 108347.

20. A. S. Iskhakov, N. T. Dinh, V. C. Leite *et al.,* Prog. Nucl. Energy **163** (2023) 104809.

21. E. M. J. Komen, A. Mathur, F. Roelofs *et al.,* Nucl. Eng. Des. **401** (2023) 112082.

22. Y. Bartosiewicz, Nucl. Eng. Des. **382** (2021) 111362.

23. S. Yang, U. Bieder, E. Studer, Nucl. Eng. Des. **414** (2023) 112543.

24. O. Bovati and Y. Hassan, Nucl. Eng. Des. **414** (2023) 112587.

25. D. M. Pérez, A. G. Rodríguez, L. H. Pardo *et al.*, Int. J. Thermodyn. **24** (2021) 125.

26. D. M. Pérez, D. M. Pérez, L. H. Pardo *et al.*, Int. J. Thermodyn. **24** (2021) 9.

27. ANSYS, Best Practice: Scale-Resolving Simulations in Ansys CFD, 2021.

28. F. R. Menter, R. Sechner, A. Matyushenko, Best Practice: RANS Turbulence Modeling in Ansys CFD, St. Petersburg, 2021.

29. G. Haller, J. Fluid Mech. **525** (2005) 1.